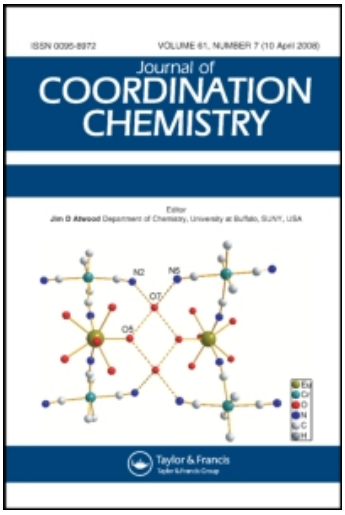

Journal of Coordination Chemistry
Publication details, including instructions for authors and subscription information:
http://www.informaworld.com/smpp/title~content=t713455674

COORDINATION OF $CU^{2\pm}$ BY MONO-AMINOALKYLOXAMIDES IN AQUEOUS SOLUTION

Sieglinde Cattoir[a]; Gerrit G. Herman[a]; André M. Goeminne[a]
[a] Laboratory for General and Inorganic Chemistry, University of Ghent, Ghent, Belgium

To cite this Article Cattoir, Sieglinde , Herman, Gerrit G. and Goeminne, André M.(1996) 'COORDINATION OF $CU^{2\pm}$ BY MONO-AMINOALKYLOXAMIDES IN AQUEOUS SOLUTION', Journal of Coordination Chemistry, 40: 1, 83 — 102
To link to this Article: DOI: 10.1080/00958979608022848
URL: http://dx.doi.org/10.1080/00958979608022848

J. Coord. Chem., 1996, Vol. 40, pp. 83–102
Reprints available directly from the publisher
Photocopying permitted by license only

COORDINATION OF Cu^{2+} BY MONO-AMINOALKYLOXAMIDES IN AQUEOUS SOLUTION

SIEGLINDE CATTOIR, GERRIT G. HERMAN* and ANDRÉ M. GOEMINNE

Laboratory for General and Inorganic Chemistry, University of Ghent, Krijgslaan 281 (S3), B-9000 Ghent, Belgium

(Received 11 January 1996)

Complex formation equilibria of Cu^{2+} complexes of *N*-(2-aminoethyl)oxamide, *N*-(3-aminopropyl)oxamide, 1, 8-diamino-3, 6-diazaoctane-7, 8-dione and 1, 10-diamino-4, 8-diazaoctane-9, 10-dione in aqueous solution at 25°C ± 0.1°C and I = 0.1 mol dm^{-3} (KNO_3) have been studied using potentiometric and spectrometric titrimetry. Mixed ligand titrations using 2, 2'-bipyridyl as the second ligand have been added in order to obtain unambiguous results. The Cu^{2+} complexes of the monoalkyl substituted oxamides studied can be classified into three groups: (1) $CuLH_{-1}$ and $CuLH_{-2}$ complexes; these complexes have a single deprotonated oxamide group in a *trans* configuration; (2) a $CuLH_{-3}$ complex; this complex has a doubly deprotonated oxamide group in a *cis* configuration; (3) Cu_2LH_{-2}, $Cu_3L_2H_{-4}$ and $Cu_3L_2H_{-5}$ complexes; these polynuclear complexes have the doubly deprotonated oxamide group in a *trans* configuration. Deprotonation of the primary amide group in the Cu_2LH_{-2} complex of these ligands occurs before pH = 5. This unprecedented deprotonation of a primary amide group under these conditions is due to the cooperation of both strong and optimally positioned coordinating groups. The concept of amide oxygen anchoring is introduced.

Keywords: aminoalkyloxamides; protonation; stability constants; copper(II)

INTRODUCTION

The coordination properties of the oxamide group have been investigated extensively.[1–9] The unsubstituted oxamide group, although used succesfully as a bridging ligand, is not able to coordinate any metal ion under mild conditions in aqueous solution.[10]

* Author for correspondence.

In weakly acidic conditions, doubly substituted oxamide group bearing aminoethyl-, aminopropyl-, acetyl- or 2-pyridiniummethyl- substituents primarily forms a binuclear metal ion complex as shown for *N,N'*-bis(2-aminoethyl)oxamide. This type of binuclear complex is clearly due to the symmetry of such ligands; both amide groups can be deprotonated and coordinated due to the assistance of the optimally placed amino groups.

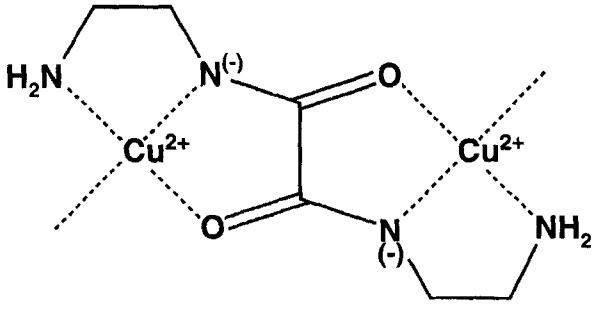

The deprotonation and complexation of oxamide nitrogens under mild pH conditions is expected to be assisted by the amino group nitrogen or carboxylate oxygen anchors in substituents. Other coordination modes resulting in weaker complexes might be used if only one of the oxamide nitrogens is substituted. The ligands used to represent a class of mono-substituted oxamides are *N*-(2-aminoethyl)oxamide (L^1), *N*-(3-aminopropyl)oxamide (L^2), 1,8-diamino-3,6-diazaoctane-7,8-dione (L^3) and 1,10-diamino-4,8-diazaoctane-9,10-dione (L^4). Their chemical structures are represented below.

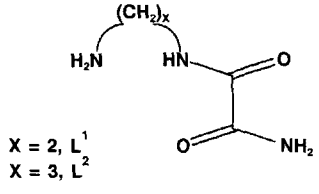

X = 2, L^1
X = 3, L^2

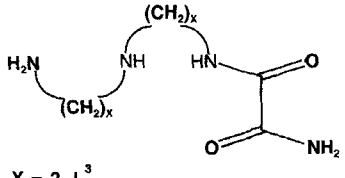

X = 2, L^3
X = 3, L^4

EXPERIMENTAL

Reagents

All chemicals were of analytical grade and used as received.

Solutions

Distilled and deionised water (Milli-Q quality, conductance < 0.05 mS cm^{-1}) was used throughout for all solutions. Carbonate-free (< 0.5%) potassium hydroxide solutions (*ca* 0.200 mol dm^{-3}) were prepared from Titrisol ampoules and were standardised by titration with HCl. The HCl solution was standardised by argentometry. Metal ion stock solutions were prepared from metal nitrates and were standardised by titration with the disodium salt of ethylenediaminetetraacetic acid (edta) in the presence of a small amount of the Hg(edta) complex using appropriate conditions and electrodes (mercury and calomel electrode).[11] All final solutions for the potentiometric and spectrophotometric titrations were made up to an ionic strenght of 0.1 mol dm^{-3} with potassium nitrate.

Synthesis of L^1 and L^2

L^1 was obtained by slowly adding ethyl oxamate (1.0 mol) to 1,2-diaminoethane (15.0 mol) at room temperature. L^2 was obtained in a similar way, using 1,3-diaminopropane instead of 1,2-diaminoethane. The solution was filtered and the excess amine was distilled off under reduced pressure. The residue was dissolved in methanol and recrystallised from methanol/ether (yield 80%). Anal., mass (Riber 10-10B quadrupole mass spectrometer, CI) *m/z* 132 for L^1 (MH^+) and *m/z* 146 for L^2 (MH^+); IR (Brücker IFS 113 V FT-spectrometer) 3312 cm^{-1}(ν (NH), strong), 1656 cm^{-1} (ν(CO), very strong), 1540 cm^{-1} (δ(NH) + n(CN), strong), for L^1; 3320 cm^{-1} (ν(NH), strong), 1656 cm^{-1} (ν(CO), very strong), 1582 (δ(NH) + ν(CN), strong) for L^2.

The amines were then converted into the corresponding hydrochloric salts. To a concentrated solution of L^1 or L^2 in ethanol was slowly added a 12 mol dm^{-3} HCl (aq) to pH = 1. The precipitate was recrystallised from 70% ethanol/water (yield 65%). The purity of the salts obtained by argentometry and pH-metry was 99.5%.

Synthesis of L^3 and L^4

L^3 and L^4 were obtained in a way analogous to that described for L^1 and L^2, using diethylenetriamine for L^3 or imino-*bis*(3-propylamine) for L^4 and ethyl oxamate

(yield 57%, 66% respectively). Anal., mass (CI) *m/z* 175 for L^3 (MH^+) and *m/z* 203 for L^4 (MH^+). The corresponding hydrochloric salts were prepared (purity 99.8% by argentometry and pH metry). ^1H NMR (Brücker WH-360 spectrometer, D_2O/DCl, DSS as reference): 3.35 ppm (t, 2H), 3.46 ppm (t, 2H), 3.48 ppm (t, 2H), 3.68 ppm (t, 2H) for L^3.2HCl; 1.95 ppm (q, 2H), 2.05 (q, 2H), 3.08 ppm (t, 2H), 3.12 ppm (t, 2H), 3.15 ppm (t, 2H), 3.40 ppm (t, 2H) for L^4.2HCl.

Potentiometric Measurements

The potentiometric measurements were carried out using a titration system equipped with a Schott CG841 pH meter and a Schott T200 burette (total volume 5 cm^3 or 10 cm^3). The pH meter was fitted with a Schott glass electrode and a Schott Ag/AgCl reference electrode with a second salt bridge filled with 0.1 mol dm^{-3} KNO_3 solution. A Schott titration assembly was used with a thermostatted vessel (50 cm^3 or 80 cm^3) and a magnetic stirrer. All titrations were performed at 25 ± 0.05°C under an atmosphere of nitrogen, presaturated with water vapour by bubbling through a 0.1 mol dm^{-3} KNO_3 solution. The program TITRATE, slightly modified, was used to monitor the titration.[12]

The electrode system was calibrated as a hydrogen ion concentration probe (pH = -log[H^+]) by titrations of hydrochloric acid (50 cm^3 0.00941 mol dm^{-3}) with standard potassium hydroxide titrant solution (*ca* 0.200 mol dm^{-3}). The concentration of HCl was determined by argentometry. The titration data were processed using Gran's method in order to calculate the standard cell potential (E°), the dissociation of water (K_w), together with the correction terms for changes in the liquid junction potential in strong acid medium, a_j (-log[H^+]<2.5) and for the non-linear electrode response in a strong alkaline medium b_j (–log[H^+]>11.5).[13] The pK_w value was found to be 13.78 in accord with literature values, a_j = 420 m V dm^3 mol^{-1} and b_j = –90 m V dm^3 mol^{-1}.[14] The electromotoric force readings were converted into pH values using equation (*1*); pH values were obtained by successive approximations taking [H^+] as zero at the start.

$$pH = (E^\circ - E + a_j[H^+] + b_j K_w [H^+]^{-1}) / S \qquad (1)$$

The value for the Nernst slope S was obtained as the slope of the plot pH_{calc} versus $E_{measured}$ for 2.5 < pH_{calc} < 4.5 and 8.0 < pH_{calc} < 11.5, and was found to be 59.0 ± 0.05 mV. Calibration parameters remained fairly constant with time.

All initial concentrations of Cu^{2+}, ligand and HCl are given in Table I. This table also includes the concentration of the KOH solution and the total number of titration points in each titration.

TABLE I Data for the potentiometric and spectrophotometric (UV-*vis*) titrations of Cu^{2+} and L^1 to L^4 at 25°C and I = 0.1 mol dm^{-3}

n°	*Cu/L*	*mmol Cu* [a]	*mmol L* [b]	*mmol H* [c]	V_0 [d]	C_{OH} [e]	*pts* [f]
L^1, pH titrations							
1			0.5390	0.7870	80	0.2116	75
2			0.4014	0.5721	80	0.2046	50
3			0.3686	0.4646	51	0.1938	56
L^2, pH titrations							
4			0.5205	0.7685	80	0.2116	73
5			0.5674	0.8287	80	0.2116	44
6			0.4070	0.5066	80	0.2097	39
L^3, pH titrations							
7			0.1617	0.4187	51	0.2034	74
8			0.3940	0.8610	50	0.1969	74
9			0.2020	0.5040	50	0.1938	75
L^4, pH titrations							
10			0.3209	0.7003	50	0.1969	52
11			0.2000	0.4870	50	0.1938	59
12			0.1587	0.4224	52	0.2034	59
Cu^{2+} and L^1 pH titrations							
13	1/2	0.2056	0.4014	0.5721	80	0.2046	107
14	2/3	0.2056	0.3011	0.4291	80	0.2046	93
15	1/1	0.4112	0.4281	0.6340	80	0.2046	130
Cu^{2+} and L^2 pH titrations							
16	1/2	0.2056	0.4150	0.5960	80	0.2046	84
17	1/1	0.4112	0.4150	0.5960	80	0.2046	103
Cu^{2+} and L^3 pH titrations							
18	1/2	0.0557	0.1182	0.2582	50	0.1969	97
19	1/2	0.1114	0.2363	0.5163	50	0.1969	73
20	1/1	0.1114	0.1182	0.2582	50	0.1969	94
21	1/1	0.2228	0.2363	0.5163	50	0.1969	126
22	2/1	0.2836	0.1481	0.3433	50	0.1935	70
Cu^{2+} and L^4 pH titrations							
23	1/2	0.0819	0.1926	0.4200	50	0.1969	122
24	1/1	0.1782	0.1962	0.4200	50	0.1969	109
Cu^{2+} and L^1 UV-vis titrations (cellength = 2 cm)							
25	1/2	0.0587	0.1157	0.1405	20	0.2097	12
26	2/3	0.2830	0.3790	0.3790	50	0.2100	9
27	1/1	0.2830	0.3030	0.3030	50	0.2100	12
Cu^{2+} and L^2 UV-vis titrations (cellength = 2 cm)							
28	1/2	0.0587	0.1163	0.1447	20	0.2097	13
29	1/1	0.0587	0.0582	0.0724	20	0.2097	10
Cu^{2+} and L^3 UV-vis titrations (cellength = 1 cm)							
30	1/1	0.0148	0.0164	0.0358	5	0.1969	10
31	1/1	0.1542	0.1617	0.3234	40	0.2243	22
Cu^{2+} and L^4 UV-vis titrations (cellength = 1 cm)							
32	1/1	0.1782	0.1926	0.4200	60	0.1969	10
33	1/1	0.1928	0.1984	0.3967	50	0.2034	30

[a]mmolCu: number of millimoles Cu^{2+} in the initial solution. [b]mmolL: number of millimoles ligand in the initial solution. [c]mmolH: number millimoles H+ in the initial solution. [d]V_0 : initial volume in cm^3. [e]C_{OH}; concentration KOH titrant in mol dm^{-3}. [f]Pts: total number of data points.

Formation Curves

Formation curves were used in the chemical/mathematical analysis of complete complex formation of L^1 and L^2 with Cu^{2+}. Mathematical difficulties deriving from the missing second and third deprotonation constant of these ligands (pK_{-1} and pK_{-2}) are by-passed in the same way as described in a previous paper.[15] Thus $\bar{n}$ is plotted *versus* pL-pH (instead of $\bar{n}$ *versus* pLH_{-1}) and this formation curve is shifted by the value of pK_{-1} to the actual formation curve.

In the case of L^3 and L^4, we also used visible absorbance data to obtain the formation curve for a 'MLH $\rightleftharpoons$ ML + H' type of equilibrium. The absorbance at a specific wavelength for all spectra recorded in this buffer region and the corresponding pH values are used to obtain this formation curve. The absorbance for 0% ML complex formation is set at 0 and for 100% ML complex formation at 1. All intermediate absorbances are normalised accordingly. Plotting the pH values *versus* these corrected absorbance values gives the formation plot for the 'MLH $\rightleftharpoons$ ML + H' equilibrium.

Electronic Spectrophotometric Measurements

Electronic absorption spectra were recorded at 25°C on a Hewlett Packard 8451A diode array spectrophotometer in the wavelength region 190 to 820 nm. Consecutive spectra for systems with rapid equilibria were obtained from titrations similar to those in the potentiometric experiments; for each titration point a small amount of the titration solution was injected into a cell of appropriate length and re-injected after recording the spectrum. For systems involving slow equilibria, spectra were obtained from separate solutions for each titration point after an appropriate equilibration period. Experimental conditions for all potentiometric and spectrophotometric titrations are given in Table I.

Calculation of Equilibrium Constants

The overall stability constants β_{pqr} (= $[M_pL_qH_r]/[M]^p[L]^q[H]^r$) of the various species formed in aqueous solution were obtained from numerical analysis of all experimental emf data from the potentiometric titrations using SUPERQUAD.[16–17] Titration data obtained at different ligand to metal ratios and/or different initial concentrations of both ligand and metal were evaluated by assuming all feasible complexation models. The best models were selected after successive attempts according to the best agreement between observed and calculated data and by means of an accurate statistical analysis of the global σ-value for the refinement, the goodness of fit (χ^2) and the standard deviation of each formation constant as calculated by SUPERQUAD.

Moreover, each complex added to the model was chemically plausible.[18] The program EQUIL was used to calculate simulated titration curves for a given set of species and stability constants.[19]

RESULTS AND DISCUSSION

Protonation Constants

Some 77 to 150 data points of three titrations were used for the calculation of the protonation constants of L^1 to L^4. The protonation constants were refined using the program SUPERQUAD and are given in Table II.

Cu^{2+} Complexes

Figures 1 and 2 show selected titration curves for L^1 to L^4. All titration curves in Figure 2 clearly show two distinct buffer regions with sharp inflection points, whereas the slope at the inflection points of the L^1 and L^2 curves in Figure 1 is much smaller. Since all potentiometric titrations proceeded in a similar way, the spectra of only one of these titrations (titration n°33, Cu^{2+}:L^4 = 1:1) are shown in Figure 3. Mixed-ligand titrations using 2,2′-bipyridyl (biPy) as the second ligand, were necessary to complete this study. These mixed-ligand titrations are also followed spectrometrically. Experimental data for these titrations are given in Table II.

TABLE II Data for the potentiometric and spectrophotometric titrations of Cu^{2+} with L^1 to L^4 and 2,2′-bipyridyl (biPy) at 25°C and I = 0.1 mol dm^{-3}

n°	*L*	*mmol Cu*[a]	*mmol L*[b]	*mmol H*[c]	*mmol biPy*[d]	V_0[e]	C_{OH}[f]	*pts*[g]
pH titrations								
34	1	0.3000	0.1534	0.2457	0.1500	40	0.2002	146
35	2	0.3000	0.1538	0.2566	0.1500	40	0.2002	96
36	3	0.3000	0.1565	0.4015	0.1500	40	0.2002	113
37	4	0.3000	0.1517	0.3907	0.1500	40	0.2002	123
UV-*vis* titrations (cellength = 2 cm)								
38	1	0.3000	0.1534	0.2457	0.1500	40	0.2002	16
39	2	0.3000	0.1538	0.2566	0.1500	40	0.2002	31
40	3	0.3000	0.1565	0.4015	0.1500	40	0.2002	25
41	4	0.3000	0.1517	0.3907	0.1500	40	0.2002	19

[a] mmolCu: number of millimoles Cu^{2+} in the initial solution. [b] mmolL: number of millimoles ligand in the initial solution. [c]mmolH: number of millimoles H^+ in the initial solution. [d] mmolbiPy: number of millimoles 2,2′bipyridyl in the initial solution. [e] V_0: initial volume in cm^{-3}. [f] C_{OH}: concentration KOH titrant in mol dm^{-3}. [g]Pts: total number of data points.

Normally it would be possible to derive the stoichiometry of the apparent principal complexes from the inflection points of the titrations. This model would then be refined using the potentiometric data and SUPERQUAD and the final model would be tested using the spectroscopic data. Unfortunately this procedure cannot be followed in the case of L^1 and L^2, since the titration curves of Cu^{2+} and these ligands do not show sharp inflection points. Therefore, another procedure had to be followed. First, from the general complexation modes of the oxamide group established from previous studies on substituted oxamides, a number of Cu^{2+} complexes that should be formed by this class of substituted oxamides were proposed. Next, this group of 'principal' complexes was tested using SUPERQUAD and formation curves. These tests clearly showed that apart from the principal complexes, other complexes were present. We therefore tested a large number of extra complexes.

Using the hypothesis that the coordination properties of the oxamide group might change once this group itself is coordinated, a new coordination mode for the oxamide group was tried. This new mode was then used to add new complexes to the basic model. Finally, these new complexes were tested using SUPERQUAD and verified using the spectroscopic data and mixed-ligand titrations.

The Principal Cu^{2+} Complexes

Two coordination modes for the oxamide group in Cu^{2+} complexes are known.[10] In the first the oxamide group has its two carbonyl oxygens in a *trans* orientation, with one secondary amide group of the oxamide entity deprotonated and coordinated together with the second oxamide/oxygen. This kind of coordination is possible in weakly acidic pH conditions if the ligand contains an additional amino group in a suitable position. The coordinated amino groups act as anchors assisting in the deprotonation and coordination of the amide group. Moreover, these complexes are stabilised by the extra coordination of the amide/oxygen.[20] $CuLH_{-1}$ complexes for L^1 and L^4 having this type of oxamide coordination are depicted in Figure 4. In this way both L^1 and L^2 can also coordinate an extra hydroxide ion, which then results in the formation of a $CuLH_{-1}$ complex.

In the second mode the oxamide group has its two carbonyl oxygens in a *cis* orientation with both amide groups deprotonated and coordinated to a single Cu^{2+} ion. This coordination mode is typical for all end-on complexes of substituted oxamide ligands studied to date,[1–9] as an amide group can only act as an anchoring group for the deprotonation and coordination of a second amide group under rather extreme conditions (pH > 9). In our case this coordination mode will result in the formation of the $CuLH_{-3}$ complex for L^1, L^2 or the $CuLH_{-2}$ complex (L^3, L^4) (Figure 4). This coordination mode can also be involved in the $CuLH_{-2}$ complex for L^1 and L^2 if a water molecule occupies the fourth equatorial position

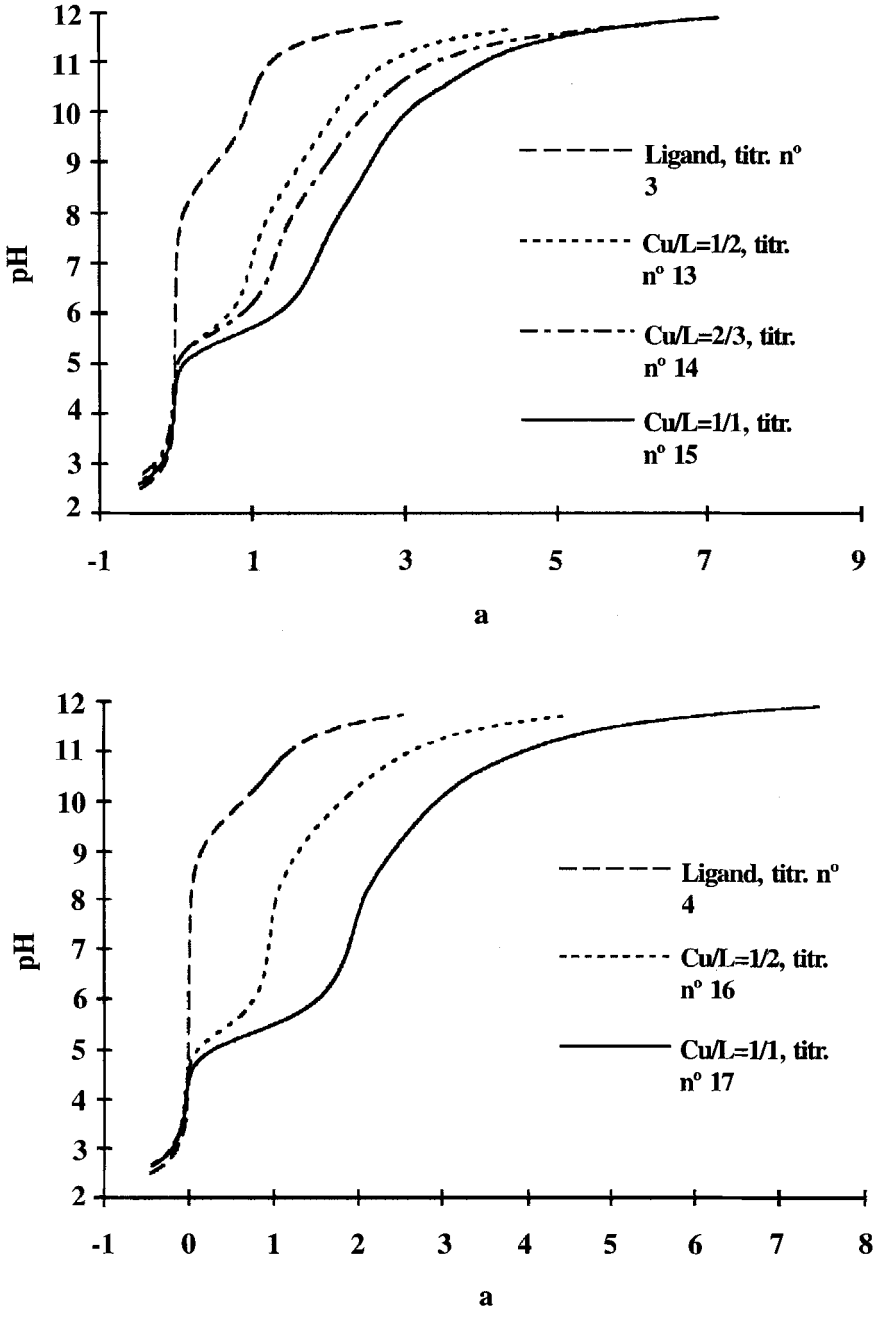

FIGURE 1 Potentiometric titrations Cu^{2+} and L^1 (upper part) or L^2 (lower part) : a selection of the titrations of Table I at 25°C and I = 0.1 mol dm^{-3}.

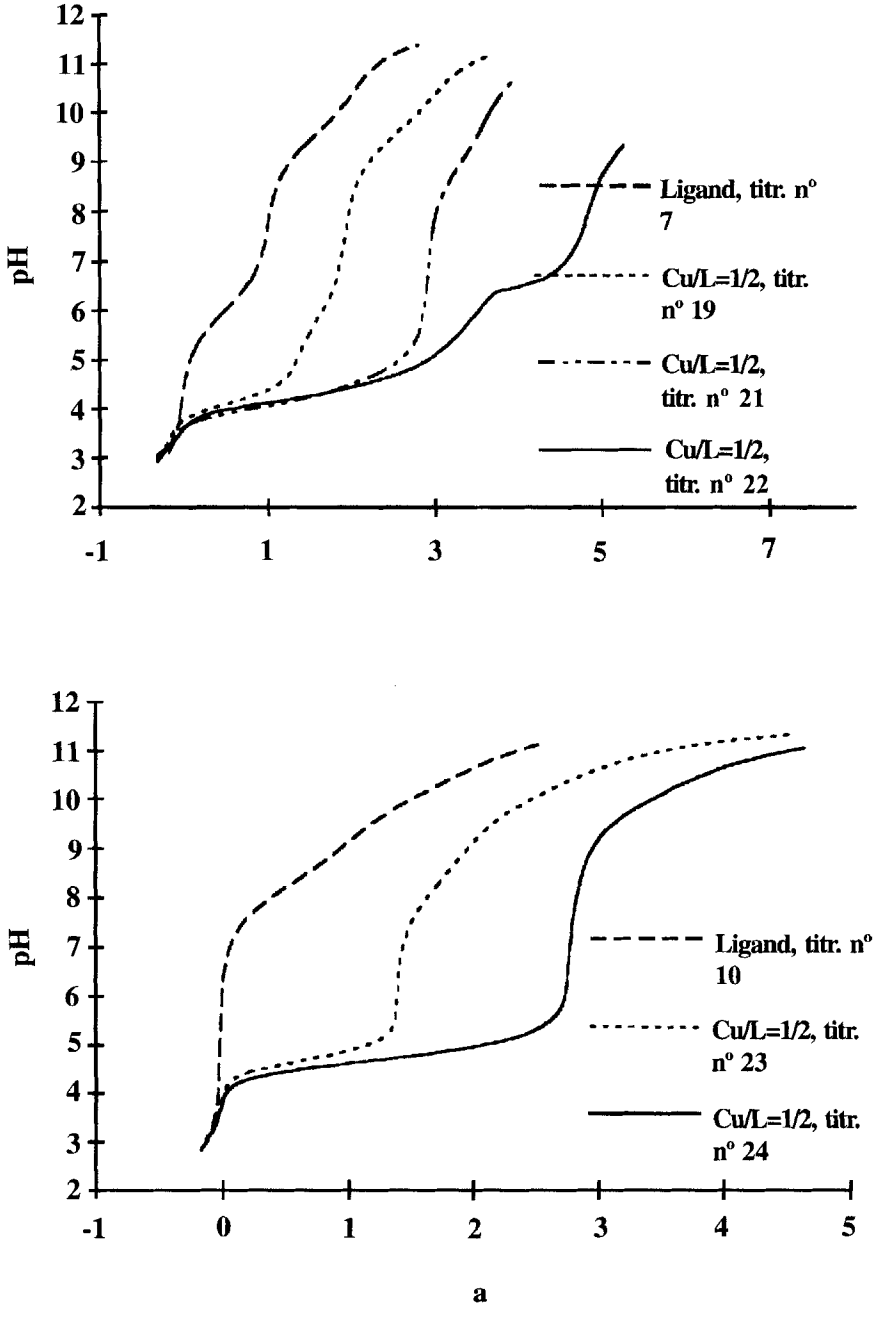

FIGURE 2 Potentiometric titrations Cu^{2+} and L^3 (upper part) or L^4 (lower part) : a selection of the titrations of Table I at 25°C and I = 0.1 mol dm^{-3}.

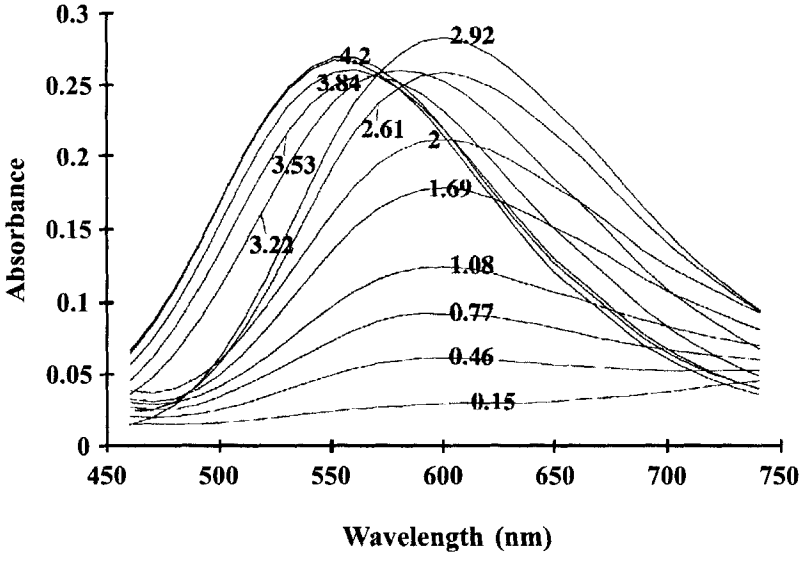

FIGURE 3 Electronic spectra recorded in titration n° 33 for Cu^{2+} and L^4 $C_{Cu^{2+}}/_{CL^4}$ = 1/1). The numbers in bold, next to the spectra represent the a value reached in the titration.

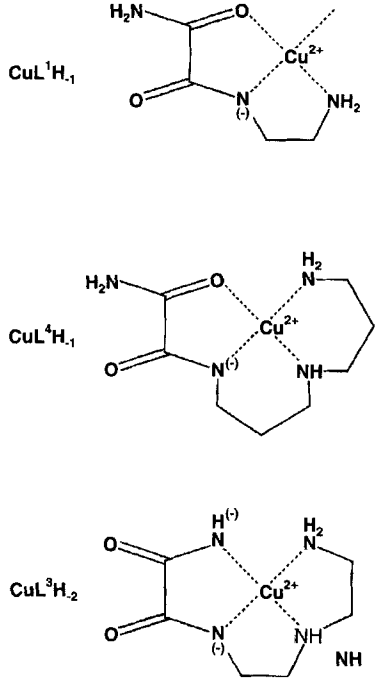

FIGURE 4 Representation of the CuL^1H_{-1}, CuL^4H_{-1} and CuL^3H_{-2} complexes.

of the Cu^{2+} centre in the complex instead of an OH-group, as is the case in CuL^1H_{-3} and CuL^2H_{-3}. The $CuLH_{-2}$ complex of glycylglycylamine, studied by Dorigatti and Billo,[21] has the second coordination mode.

The Extra Cu^{2+} Complexes

The set of principal complexes ($CuLH_{-1}$, $CuLH_{-2}$ and $CuLH_{-3}$ for L^1 and L^2; $CuLH_{-1}$ and $CuLH_{-2}$ for L^3 and L^4) was subjected to careful examination, using the data of titrations n°13 to 24 and SUPERQUAD. The set of complexes resulted in high σ-values, χ^2-values and high standard deviations for all stability constants. This is also shown in Figure 5, where the best fit for titration n°15 (Cu^{2+}: L^1=1:1) using the present set of complexes and the experimental curve are superimposed.

To pin point the problem, the formation curves for the first buffer region of titration n°15 for Cu^{2+} and L^1 and of titration n°17 for L^2 were calculated. As $CuLH_{-1}$ is the only complex from the basic set formed in the first buffer region, the experimental formation curve should fit the formation curve for a single mononuclear complex.[22] Figure 6 however clearly shows a discrepancy between theory and experiment when the degree of complexation is larger than 60%. Also, the

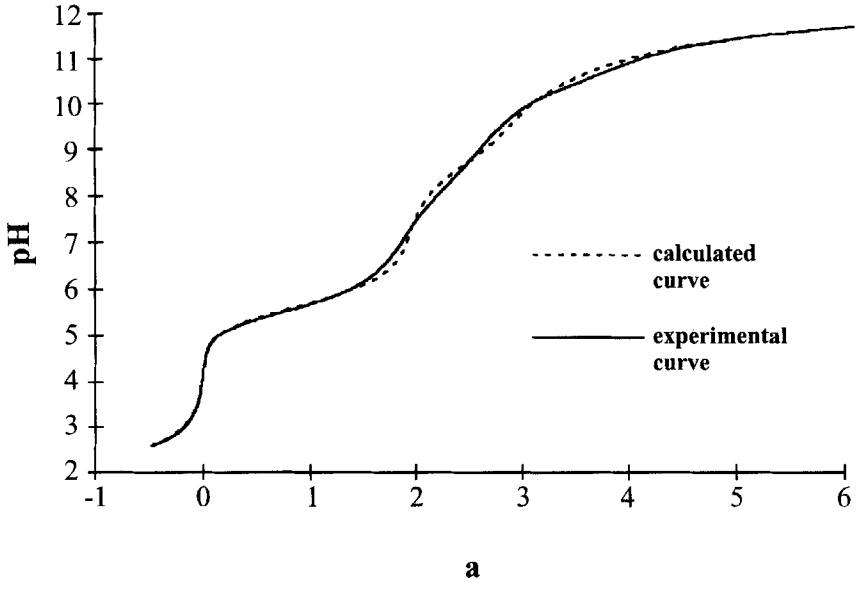

FIGURE 5 Experimental and calculated titration curve for titration n°15. Calculations were carried out for the first set of complexes proposed.

spectra from titrations n°25 to 33 cannot be interpreted by the basic set of complexes; isosbestic points are missing or should occur at different a values according to the distribution curves calculated for this set. Undoubtedly, extra complexes needed to be added to the model despite the limited number of coordination modes.

Using their primary and, if possible, secondary amino groups, L^1 and L^2 could act as monodentates, and L^3 and L^4 could act as bidentates. It should be pointed out that this mode is rejected in all complexation models of analogous ligands, since in the presence of an anchoring amino group at two or three carbon atoms distance, the amide group can easily be deprotonated, resulting in a stronger metal ligand bond, compared to an amino-copper bond.[10] This coordination mode might be used to add complexes such as CuL, CuL_2, CuL_3 and CuL_2H_{-1}. However, these extra complexes are, in all possible combinations, rejected by SUPERQUAD or result in even poorer fits to the experimental titration curves.

Oxamide Oxygen Anchoring

Complexation and deprotonation of an amide nitrogen increases the $\log K^H$ value of the corresponding amide oxygen. Increases by 2.4 log units of the $\log K^H$ values are not uncommon.[10,23–24] On the other hand, coordination of an amide oxygen must lower the pK_a value of the corresponding amide nitrogen if this nitrogen is still uncoordinated. Therefore the possibility of coordinating a second Cu^{2+} ion at the 'back' of the oxamide group of the $CuLH_{-1}$ complexes of these ligands should be considered. This would result in deprotonation and coordination of the primary amide nitrogen. In all complexes formed this way, the

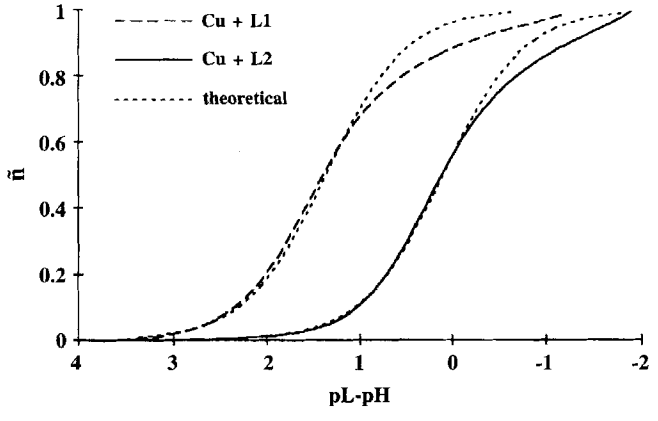

FIGURE 6 Formation curves for the first buffer region of titrations n°15 (Cu^{2+}/L^1 = 1/1) and n°17 (Cu^{2+}/L^2 = 1/1). The dotted lines are the theoretical formation curves for the formation of one mononuclear complex.

oxygen of the secondary amide group actually acts as anchor for the deprotonation of the second oxamide nitrogen. This is described as 'oxamide oxygen anchoring'. If it occurs, the following extra complexes can be formed: (a) Cu_2LH_{-2}, Cu_2LH_{-3}, $Cu_2L_2H_{-4}$, $Cu_3L_2H_{-5}$, $Cu_3L_2H_{-6}$ for L^1, L^2, and (b) Cu_2LH_{-1}, $Cu_3L_2H_{-1}$, Cu_2LH_{-2}, $CuLH_{-1}$, $CuLH_{-2}$ for L^3, L^4. Their structural formulae are shown in Figure 7.

Anchoring, however, can only occur if an excess of Cu^{2+} is present in solution. The small slope at the inflection point of the Cu^{2+} and L^1, L^2 titration curves (Figure 1) suggests this excess and the occurrence of oxamide oxygen anchoring in the second buffer region. In the L^3, L^4 titration curves however, the steep slope at the end of the first buffer region corresponds to the 100% formation of the $CuLH_{-1}$ complex. No excess of Cu^{2+} is present in the second buffer region and $Cu_3L_2H_{-4}$ cannot be formed.

These new complexes were tested, in all combinations, using titrations n°13 to 24 and SUPERQUAD. This resulted in optimum fits for the following sets: (a) for L^1, L^2 : Cu_2LH_{-2}, $Cu_3L_2H_{-4}$, $Cu_3L_2H_{-5}$, $CuLH_{-1}$, $CuLH_{-2}$, $CuLH_{-3}$ (Cu^{2+} with L^1 : 67 pts, $\sigma = 2.7$; Cu^{2+} with L^2 : 62 pts, $\sigma = 2.3$), and (b) for L^3, L^4 : Cu_2LH_{-1}, Cu_2LH_{-2},

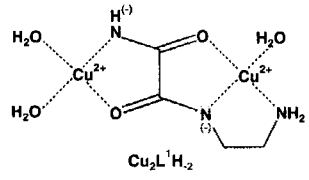

$Cu_2L^1H_{-2}$

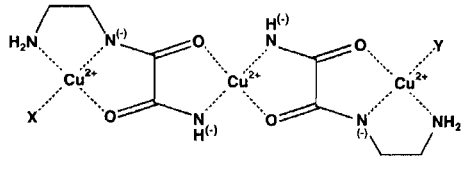

X=Y=H_2O, $Cu_3L^1{}_2H_{-4}$; X=H_2O, Y=OH^-, $Cu_3L^1{}_2H_{-5}$

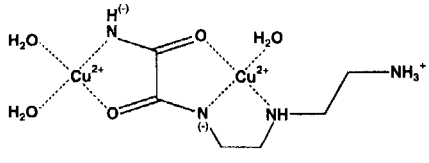

$Cu_2L^3H_{-1}$

FIGURE 7 Representation of the $Cu_2L^1H_{-2}$, $Cu_3L^1{}_2H_{-4}$, $Cu_3L^1{}_2H_{-5}$ and $Cu_2L^3H_{-1}$ -complexes.

TABLE III Stability constants, λ_{max} ε_{max}, ν_{max} values of the Cu^{2+} complexes of L^1 to L^4 at 25°C and I = 0.1 mol dm^{-3}

Ligand	*pqr*[a]	*log*β[b]	λ_{max}[c]	ν_{max}[d]	ε_{max}[e]
L^1	011	8.903(2)			
	11–1	−0.50(3)	650	15400	119
	11–2	−8.826(8)			
	11–3	−19.279(8)	574	17400	86
	21–2	−3.08(2)			
	32–4	−7.51(5)			
	32–5	−15.28(3)			
L^2	011	9.805(1)			
	11–1	0.97(2)	642	15600	66
	11–2	−8.09(1)			
	11–3	−19.00(1)	558	17900	54
	21–2	−1.77(8)			
	32–4	−5.3(1)			
	32–5	−13.65(6)			
L^3	011	9.397(3)			
	012	19.647(8)			
	11–1	5.14(2)	600	16700	159
	21–2	3.63(4)			
	11–2	−4.13	548	18250	119.3
L^4	011	5.961(5)			
	012	14.331(1)			
	11–1	6.676(4)	600	16700	78
	21–2	4.27(2)			
	11–2	−3.474	554	18050	73.5

[a]Species $M_pL_qH_r$ are indicated by their pqr code. [b]Relative standard deviations are given in parentheses.[c]In nm.[d]In cm^{-1}.[e]In L mol^{-1} cm^{-1}.

$CuLH_{-1}$, $CuLH_{-2}$ (Cu^{2+} with L^3 : 96 pts, σ = 5.3; Cu^{2+} with L^4 : 52 pts, σ = 2.2). Table III gives the corresponding stability constants. The high σ values for the Cu^{2+} with L^3 system is due to low pH values at the beginning of the first buffer region.

Because of the high pH values of the second buffer region of the Cu^{2+} with L^3 or L^4 titrations, the stability constants of the $CuLH_{-2}$ complex could not be calculated using SUPERQUAD. According to our present complex model only one complex equilibrium ($[CuLH_{-1}]^+ \leftrightharpoons [CuLH_{-2}] + H^+$) occurs in the second buffer region. Formation curves for this buffer region are then calculated using the spectrophotometric data as described earlier (Figure 8). The pK_a values derived from these formation curves and the stability constant of the $CuLH_{-1}$ complex are used to obtain the stability constant of the end complexes given in Table III. Table III also lists the ε_{max} and σ_{max} values of the $CuLH_{-1}$ complexes and the end complexes, taking into account the occurrence of the other complexes in solution. Mixed-ligand titrations with 2,2′-bipyridyl (biPy) were performed for all ligands. If oxamide oxygen anchoring occurs, it should be possible to form two mixed ligand complexes for each of these ligands :

$Cu_2LbiPyH_{-2}$ and $Cu_2LbiPyH_{-3}$ for L^1 and L^2; $Cu_2LbiPyH_{-1}$ and $Cu_2LbiPyH_{-2}$ for L^3 (Figure 9) and L^4. On the other hand, if oxamide oxygen anchoring does not occur, these complexes cannot be formed and the mixed ligand titrations could be simulated using the stability constants of the other complexes. Figure 10 shows the experimental and simulated mixed-ligand titration of Cu^{2+}, biPy and L^4 (titration n°37). The deviation between the calculated and the experimental mixed-ligand titration is in agreement with the formation of mixed-ligand complexes and consequently proves the occurrence of oxamide oxygen anchoring. In fact, we were able to calculate the stability constants of these mixed-ligand complexes using SUPERQUAD. The best fit titration curve for this minimisation (the complete set of stability constants of Table III were fixed, while the stability constants of the mixed-ligand complexes were minimised) is shown in Figure 10. There is excellent agreement between the experimental and calculated curves for $0 < a < 4$ where the mixed-ligand complexes are formed. The deviation beyond $a = 4$ is due to the presence of the CuL^4H_{-2} complex which was not included in the mixed-ligand complexation model. One could argue that another type of mixed-ligand complexes can be formed with biPy : mixed ligand complexes having a *cis* oriented oxamide group. In fact, Shu-Lin *et al.*[25] found these kind of complexes for Cu^{2+} with *N,N'*-bis(2-aminoethyl)oxamide.

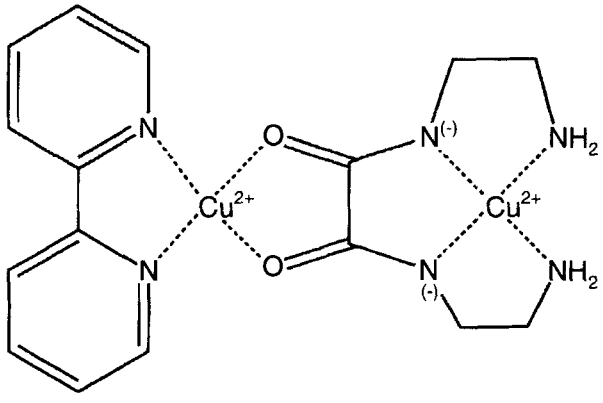

However, by use of the electronic spectra of the mixed-ligand titrations n°38 to 41, this possibility can be rejected here. For example, the spectra of titration n°41, for Cu^{2+}, biPy and L^4, are shown in Figure 11. The bold numbers correspond to the a value reached in the titration. In the spectrum taken at $a = 4$ where the mixed ligand complex, $Cu_2L^4biPyH_{-2}$ is formed maximally, the maximum wavelength is 600 nm, corresponding to the λ_{max} value for CuL^4H_{-1} having the $Cu(2N,N^-,=O)$ chromophore (λ_{max} = 600 nm and ε_{max} = 78 M^{-1} cm^{-1}). This

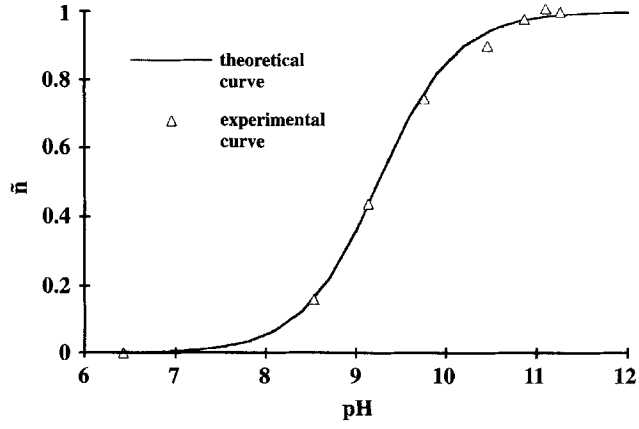

FIGURE 8 Formation curve for the second buffer region of titration n°15 (Cu^{2+}/L^1 = 1/1). The dotted line is the theoretical formation curve for the formation of one mononuclear complex.

chromophore occurs twice in the $Cu_2L^4biPyH_{-2}$ complex, assuming that the oxamide group is in a *trans* orientation. In fact, the maximum absorbance of the spectrum in Figure 11 at a = 4 is twice as high as if only CuL^4H_{-1} were 100% formed. If the oxamide group were in a *cis* configuration, the first chromophore in the $Cu_2L^4biPyH_{-2}$ complex would be the Cu(N,2N⁻,O) chromophore of CuL^4H_{-2} (λ_{max} = 554 nm and $\varepsilon_{600\,nm} \approx 55\ M^{-1}\ cm^{-1}$) and the second one would be a Cu(2 = O,2N) chromophore with λ_{max}>600 nm and $\varepsilon_{600\,nm} << 78\ M^{-1}\ cm^{-1}$. Therefore in the case of *cis* orientation of the oxamide group in $Cu_2L^4biPyH_{-2}$ the high values for the absorbances obtained at 600 nm, could never be reached.

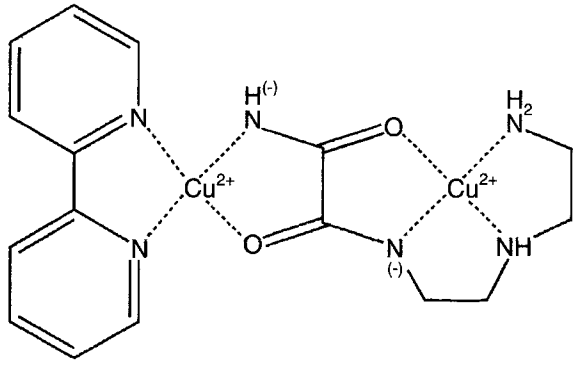

$Cu_2L^3biPyH_{-2}$

FIGURE 9 Representation of the mixed ligand complex $Cu_2L^3biPyH_{-2}$ (biPy = 2,2′-bipyridyl).

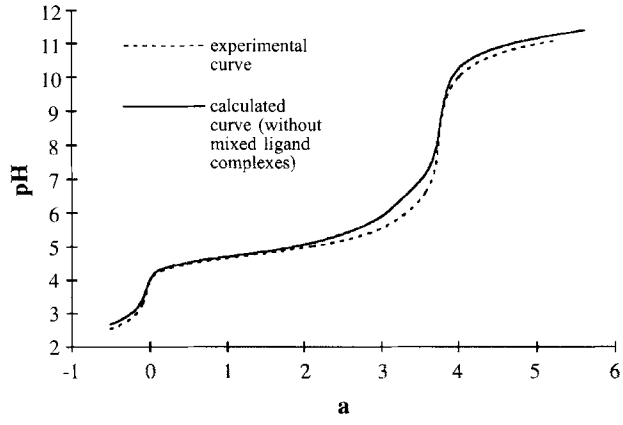

FIGURE 10 Experimental and calculated mixed-ligand titration curves for Cu^{2+}:biPy:L^1 = 2:1:1 (titration n°34, Table II); (biPy = 2,2′-bipyridyl). The upper graph is for a simulation without mixed-ligand complexes, the lower graph is for a simulation with mixed-ligand complexes.

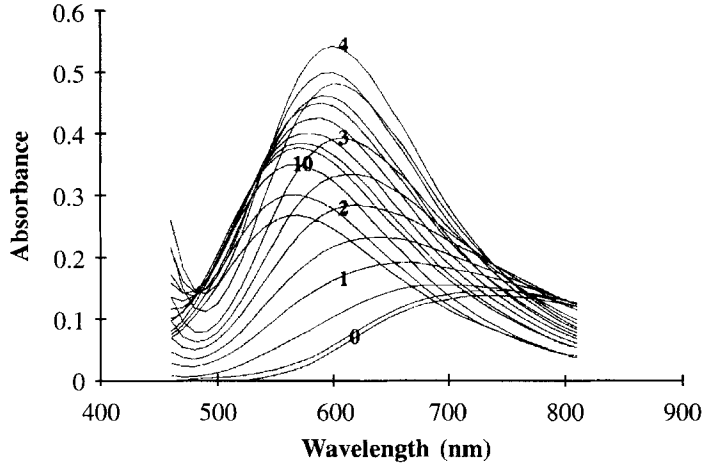

FIGURE 11 Spectra recorded in titration n°41 of Cu^{2+}:biPy:L^4 = 2:1:1 ; (biPy = 2,2′-bipyridyl). The numbers in bold, next to the spectra, represent the a value reached in the titration.

The experimental mixed-ligand titration in Figure 10 shows substantial mixed-ligand complex formation at pH < 6. Even if assisted by the bridging biPy, one can hardly assume primary amide deprotonation and complexation in weak acid conditions without the assistance of an anchoring group.

Primary amide deprotonation is brought about in these complexes at surprisingly low pH values. For Cu^{2+} and L^3 oxamide oxygen anchoring occurs at pH = 4, even before the primary ammonium group is neutralized. For the less

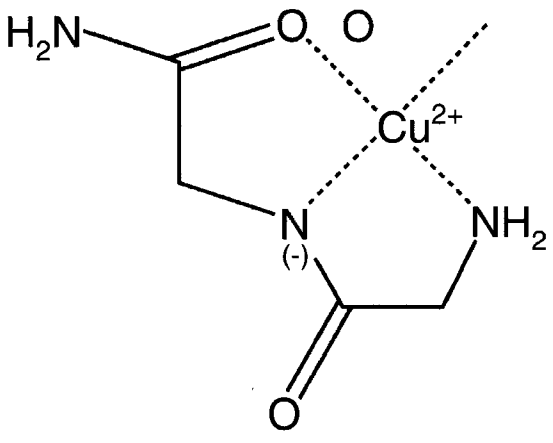

powerful ligands L^1 and L^2 possessing only one amino group, pH values about 6 are sufficient for primary amide deprotonation. It is clear that not only the type, but also the specific sequence of the different functional groups in these ligands accounts for this exceptional behaviour. Note that glycylglycinamide (GGa) and L^1, although structural isomers, do not coordinate in the same manner. According to Dorigatti and Billo[21] GGa and Cu^{2+} form four complexes : CuGGa, $CuGGaH_{-1}$, $CuGGaH_{-2}$ and $CuGGaH_{-3}$. No intermediate complexes are formed and indeed, the $CuGGaH_{-1}$ complex, shown here, does not possess a suitably placed anchor to assist in the deprotonation/complexation of the primary amide group.

Acknowledgments

The authors thank Prof. Dr. H.O. Desseyn from the University of Antwerp, RUCA, Antwerp for his kind interest in this work. One of us (G.G.H.) acknowledges a grant from the N.F.W.O. (Krediet aan Navorsers n° 31501891).

References

[1] R. Griesser and S. Fallab, *Chimia*, **22**, 90 (1968).
[2] Ojima and K. Nonoyama, *Coord. Chem. Rev.*, **92**, 58 (1988).
[3] F. Lloret, M. Julve, J. Faus, Y. Journaux, M. Philoche-Levisalles and Y. Jeannin, *Inorg. Chem.*, **28**, 3702 (1989).
[4] V.G. Albano, C. Castellari, A.G. Fabretti and A. Giusti, *Inorganica Chimica Acta*, **191**, 213 (1992).
[5] F. Lloret, J. Sletten, R. Ruiz, M. Julve, J. Fausand, M. Verdaguer, *Inorg. Chem.*, **31**, 778 (1992).
[6] F. Lloret, M. Julve, J.A. Real, J. Faus, R. Ruiz, M. Mollar, I. Castro and C. Bois, *Inorg. Chem.*, **31**, 2956 (1992).

[7] F. Lloret, M. Julve, J. Faus, R. Ruiz, I. Castro, M. Mollar and M. Philoche-Levissalles, *Inorg. Chem.*, **31,** 784 (1992).
[8] J.A. Real, M. Mollar, R. Ruiz, J. Faus, F. Lloret, M. Julve, M. Philoche-Levisalles, *J. Chem. Soc., Dalton Trans.*, 1483 (1993).
[9] J. Soto, R. Martines-Màñez, J. Payà, F. Lloret, M. Julve, *Trans. Met. Chem.*, **18**, 69 (1993).
[10] H. Sigel and R.B. Martin, *Chem. Rev.*, **82**, 385 (1982).parentheses.[c]In nm.[d]In cm^{-1}.[e]In L mol^{-1} cm^{-1}.
[11] A.I. Vogel, *A Text-book of Quantitative Analysis*, p.959 (Longrams and Green, New York, 1961).
[12] A.P. Arnold, S.A. Daignault and D.L. Rabenstein, *Anal. Chem.*, **57**, 1112 (1985).
[13] G. Gran, *Analyst (London)*, **77**, 661 (1952).
[14] A.E. Martell and R.M. Smith, *Critical Stability Constants,* Vol. **6** (Plenum Press, New York (1985).
[15] S. Cattoir, G.G. Herman, A.M. Goeminne, H. Dessyn, *J. Coord. Chem.*, **38**, 245 (1996).
[16] A. Sabatini, A. Vacca and P. Gans, *Coord. Chem. Rev.*, **120**, 398 (1992).
[17] P. Gans, A. Sabatini and A. Vacca, *J. Chem. Soc., Dalton Trans.*, 1195 (1985).
[18] E. Leporati, *J. Coord. Chem.*, **33**, 179 (1994).
[19] I. Ting-Po and G.M. Nancollas, *Analyt. Chem.*, **44**, 1940 (1972).
[20] A. Zuberbühler, S. Fallab, *Helv. Chim. Acta*, **50**, 889 (1967).
[21] T.F. Dorigatti, E.J. Billo, *J. Inorg. Nucl. Chem.*, **37**, 1515 (1976).
[22] F.J.C. Rossotti and N. Rossotti, *The Determination of Stability Constants* p. 40 (McGraw-Hill, New York, 1961).
[23] J.M.T. Raycheba, D.W. Margerum, *Inorg. Chem.*, **19**, 497 (1980).
[24] J.C. Cooper, L.F. Wong, D.W. Margerum, *Inorg. Chem.*, **17**, 261 (1978).
[25] S. Ma, D. Liao, Z. Jiang, S. Yan, G. Wang, *Polyhedron*, **13**, 1647 (1994).